A GENERIC APPROACH FOR ASSIMILATING SCATTEROMETER OBSERVATIONS

Ad.Stoffelen@KNMI.nl
http://www.knmi.nl/~stoffele

Abstract

Scatterometers provide accurate and spatially consistent near-surface wind information. Hardware permitting, there is a continuous series of scatterometers with at times ideal coverage of the ocean surface wind in the coming two decades. ERS scatterometer observations have proven important for the forecasting of dynamical weather, such as tropical cyclones. Recently, SeaWinds scatterometer measurements from QuikScat have become available. SeaWinds on QuikSCAT provides great coverage over the oceans. Quality monitoring, rain contamination, wind direction noise characteristics, and wind direction ambiguity selection are now being investigated as a necessary step towards routine and successful use in weather forecasting. The methodology developed for the successful application and assimilation of ERS winds is being generalised to include the newer scatterometer concepts, such as NSCAT and SeaWinds, as described in this paper.

Specific problems in scatterometer data assimilation include

- The non-linear relationship between backscatter and wind;
- Lack of physical understanding and the consequent use of empirical modelling;
- Rain contamination in case of Ku-band scatterometers such as NSCAT or SeaWinds;
- Wind vector solution ambiguities;

Since at each node only three or four measurements are used to determine just two variables, it is well possible to visualise the problem of scatterometer data interpretation and assimilation. This is done by making cross-sections through the 3D or 4D measurement (phase) space, where the wind domain spans a 2D surface, called "the cone". It is shown that this cone reveals information on

- The Geophysical Model Function (GMF);
- The noise of the measurements;
- The optimal wind retrieval or inversion process;
- Quality Control (QC) procedures, including rain elimination in case of NSCAT or SeaWinds;
- Backscatter and wind calibration and validation strategy;
- Ice screening procedure; and
- Data assimilation methodology;

The limited number of variables, and the general overdeterminacy of the wind vector make the scatterometer data interpretation and assimilation problem an excellent playground to study the optimal treatment of measurements that are related in a very non-linear way to the meteorological model state.

Challenges that remain in scatterometry are

- The interpretation of scatterometer observations as ocean wind stress, by investigating the sensitivity of the residual wind error to ocean currents, atmospheric stability, or waves;
- The assimilation of the high spatial resolution of scatterometer winds into NWP models and the achievement of consistent temporal and spatial high-resolution near-surface wind fields; and
- The full exploitation of the more complete coverage of SeaWinds;

1 INTRODUCTION

ERS scatterometer winds have proven to be very useful for the forecasting of dynamic weather (*Isaksen and Stoffelen*, 2000). Increased coverage, such as from tandem ERS-1 and ERS-2 measurements, clearly improve the forecasts of extreme events (e.g., *Stoffelen and Beukering*, 1998; *Le Meur et al*, 1997). Improved coverage from the Ku-band scatterometers NSCAT and SeaWinds have thus great potential (*Atlas and Hoffman*, 2000). Preliminary attempts to assimilate SeaWinds data have been carried out with mixed success and improved data characterisation and assimilation procedures are needed (*Leidner and Isaksen*, 2000; *Tahara*, 2000).

Severe storms that hit Europe often originate over the North Atlantic Ocean, where sparse meteorological observations are available. Consequently, the initial stage of severe storms is often poorly analysed and their development poorly predicted (*ESA*, 1999, *WMO*, 2000). As a result, occasional devastating ocean or coastal wind and wave conditions remain a main challenge for NWP. The SeaWinds data coverage is such that developing storms are likely hit, thus depicting their position and amplitude. Moreover, the near-surface wind conditions drive the ocean circulation that in turn plays a major role in the climate system and in ocean life (e.g., fishery).

Figure 1 presents an example, showing the high spatial resolution in the QuikScat scatterometer winds, and the aditional information content as compared to ECMWF first guess.

Besides using scatterometers, one can measure components of the wind field with Synthetic Aperture Radar (SAR) or passive radar measurements (*WindSat*, 2000; *SSMIS*, 2000). A SAR also measures the radar backscatter but at higher resolution (down to ~100 m) and at only one azimiuth. The latter is a problem since it is not possible to resolve both wind direction and speed at matching resolution without prior information (underdeterminacy). For passive radar measurements the same applies, but here the wind direction sensitivity of the measurements is so small that wind speed can be retrieved with sufficient accuracy. However, a more significant problem is that the radar measurement sensitivity to rain, cloud liquid water, and humidity has to be appropriately accounted for by using multiple frequency measurements. This somewhat limits passive radar capabilities in dynamic weather conditions (*McNally*, this issue).

In this paper we exclusively deal with scatterometer measurements. After comparing the characteristics of the different instruments, we look at the physical description of the measurement process and conclude that empirical methods are needed for modelling the Geophysical Model Function for matching the accuracy of the instrumentation. The concept of measurement (phase) space is introduced as a very effective tool for aid in controlling the interpretation and QC of scatterometer measurements. In the measurement space the GMF is represented by a twodimensional (2D) non-linear surface, called "cone". The uncertainties in the instrument, GMF, spatial representation, and wind forecast model are the main concern in GMF estimation, GMF inversion for wind retrieval, and data assimilation. The non-linear transformation of these error distributions between the wind and the backscatter domain is of fundamental concern. For example, it makes that the assimilation of retrieved winds is more effective than the assimilation of backscatter data. A generic approach for the assimilation of scatterometer winds is presented here.

In scatterometer data assimilation (*Stoffelen, Voorrips, and de Vries*, 2000), the following needs to be considered:

- ocean backscatter calibration and validation (e.g., *Stoffelen*, 1999; *Stoffelen and Anderson*, 1998; *Stoffelen*, 1997; *Stoffelen and Beukering*, 1997; and *Figa and Stoffelen*, 1999);
- wind retrieval algorithm (e.g., *Stoffelen and Anderson*, 1998 and 1993; *Figa and Stoffelen*, 2000);
- wind and radar backscatter quality control algorithms (*Stoffelen and Anderson*, 1998 and 1997; *Stoffelen and Beukering*, 1997;
- including rain detection (*Figa and Stoffelen*, 2000; *Portabella and Stoffelen*, 2000);
- ambiguity removal (*Stoffelen and Anderson*, 1997; *de Vries and Stoffelen*, 2000); and
- monitoring methodology (*Stoffelen*, 1998b; *Le Meur et al*, 1998);

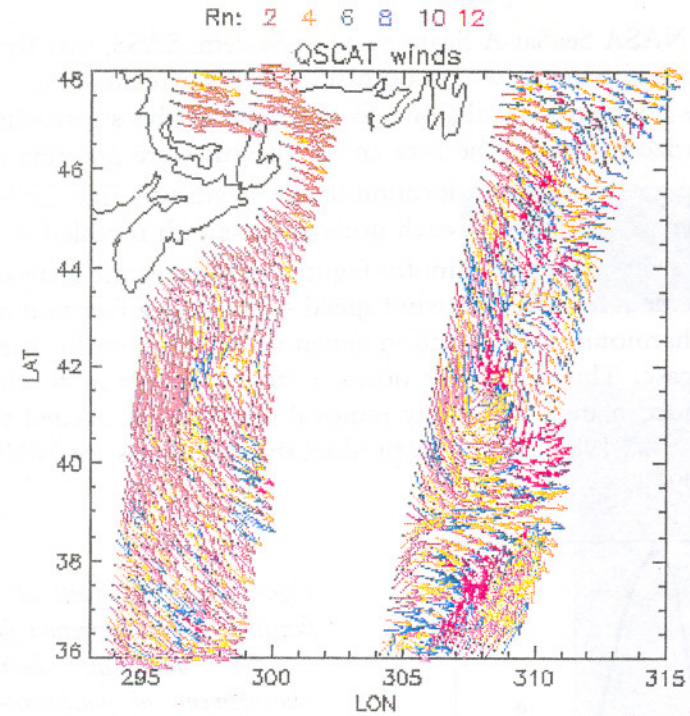

Figure 1.a: QuikScat winds in the Atlantic in the development zone of the devastating storms that hit Western Europe during Christmas 1999. Date and time of observation are December 24 22 GMT. The inversion residual is normalised as a function of speed and WVC, such that a number Rn results with an expectation value of one. Rn values for good quality winds between 2 and 4 are thus unlikely, and winds at values above 4 are verified to be generally of bad quality (Portabella and Stoffelen, 2000). The colour code for the Rn values is shown above the plot. Anomalous winds have generally Rn > 4. For Rn < 4 large areas remain that depict relevant and important mesoscale features of the wind field.

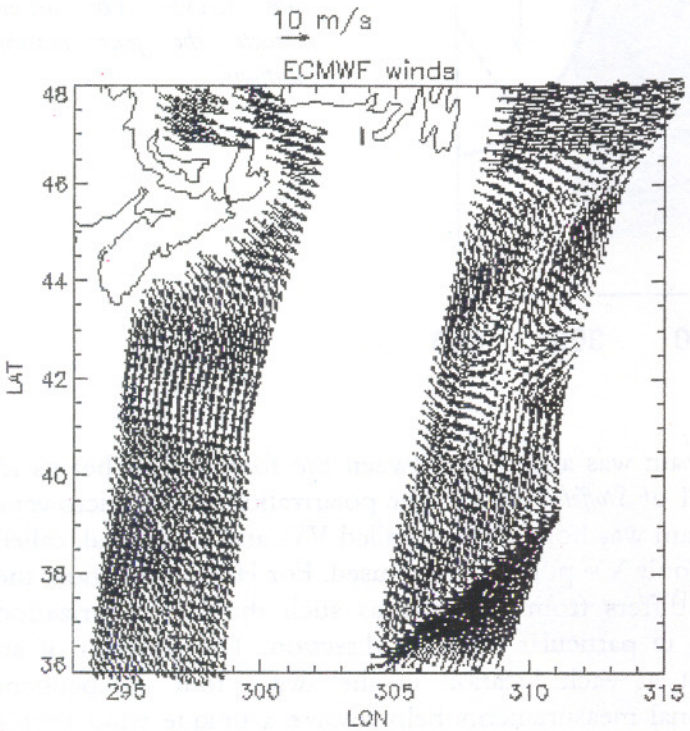

Figure 1.b: As figure 1.a, but ECMWF winds. Dynamical features particularly appearing in the right SeaWinds swath are not well represented in the ECMWF first guess, for example the through orientation and position, and the low at 308E and 41N.

I will not explicitly address all these issues here, but rather present a selection of topics that I feel are of some educational value and refer to the papers above for further reading on other topics.

2 INSTRUMENTS

2.1 SEASAT, NSCAT AND SEAWINDS

The first scatterometer in space was the NASA SeaSat-A Scatterometer System, SASS, that flew in 1978 for amply three months. SASS had four antennae, two on both sides of the satellite (*Stoffelen*, 1998; Chapter I). Each set of two antennae covered a swath; one to the right of the subsatellite (ground) track and one to the left. In the horizontal plane, the fore and aft beams were pointing at respectively 45° and 135° with respect to the ground track. A location in the swath was first hit by the fore beam, and a few minutes later by the aft beam. Thus, each node in the swath revealed two backscatter measurements obtained with a 90° difference in azimuth. Figure 2 illustrates the analysis of two such measurements. For each measurement it shows the wind speed solution as a function of all possible wind directions. Given the basic harmonic wind direction dependency of the backscatter signal, four solutions exist in this general case. This ambiguity poses a strong limitation to the usefulness of the SASS wind data, and extended manual ambiguity removal efforts were needed to obtain an acceptable wind product [*Peteherych et al.*, 1984]. With this product the usefulness for NWP could be shown (see, e.g., *Stoffelen and Cats* [1991]).

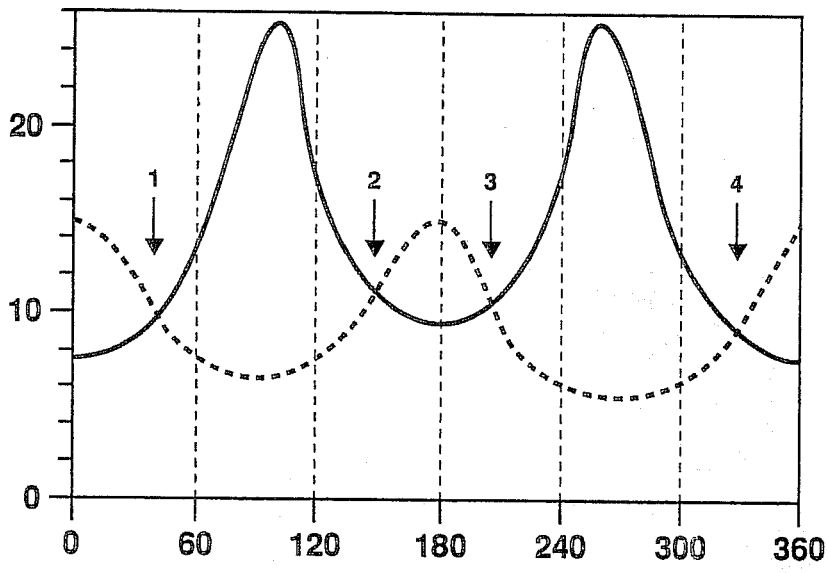

Figure 2: Wind speed as a function of wind direction for a fore and aft beam measurement of backscatter from SASS. The arrows indicate the four possible solutions.

In a follow-on design, i.e., NSCAT, a beam was added in between the fore and aft beams to both sides of the swath, as shown in chapter 1 of *Stoffelen* (1998). The polarization of the microwave radiation emitted and received by the mid beam was both vertical, called VV, and horizontal, called HH. For the other antennae and instruments only VV polarization is used. For HH polarization, the relationship between backscatter and wind differs from VV, and as such the HH polarization provides useful complementary information, in particular on wind direction. The addition of an antenna with two polarizations makes that at each location in the swath four independent measurements are available. The two additional measurements help resolve a unique wind vector solution. However, an azimuth direction of the mid beam precisely in between the azimuths of the fore and aft beams would have better sampled the harmonic wind direction dependency. This was not done for technical reasons.

NSCAT was mounted on the Japanese Advanced Earth Observation Satellite, ADEOS. After nine months with useful NSCAT data, at the end of June 1997, the Japanese space agency, NASDA, lost control of the ADEOS after a complete power loss. This dramatic event has been a severe set-back for Earth Observation, and scatterometry in particular.

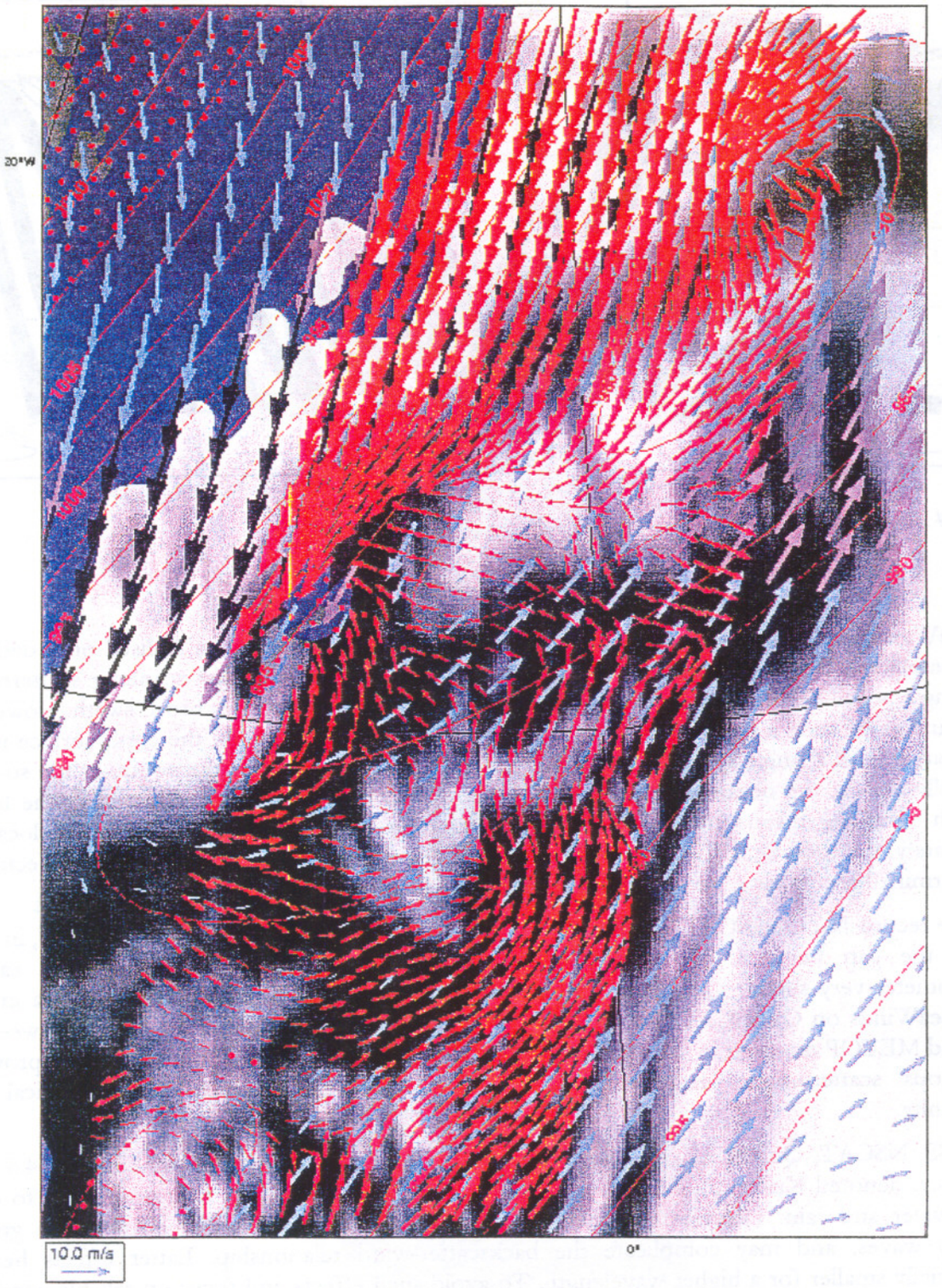

Figure 3 Scatterometer winds from ERS-2 around 12 GMT on 24/11/'99 at 70N and 0W (http://www.knmi.nl/scatterometer). The following information is displayed : Grey-shaded IR METEOSAT image coherent with the scatterometer winds. Blue mask for which the sea surface temperature is below zero degrees and where sea ice is probable. Grey mask for land presence at 80N and 20W (top is north). Red contours of surface pressure from the HIRLAM model at KNMI (3-hour forecast). Blue and purple are the spatially smooth wind vectors from HIRLAM (the amount of purple increases with wind speed). Red wind vectors depicting the spatially detailed ERS-2 winds at KNMI. At the red dots the winds were rejected because of a confused sea state (lower left) or the presence of sea ice (top left).. It remains a challenge to assimilate the spatial detail as measured by a scatterometer into NWP.

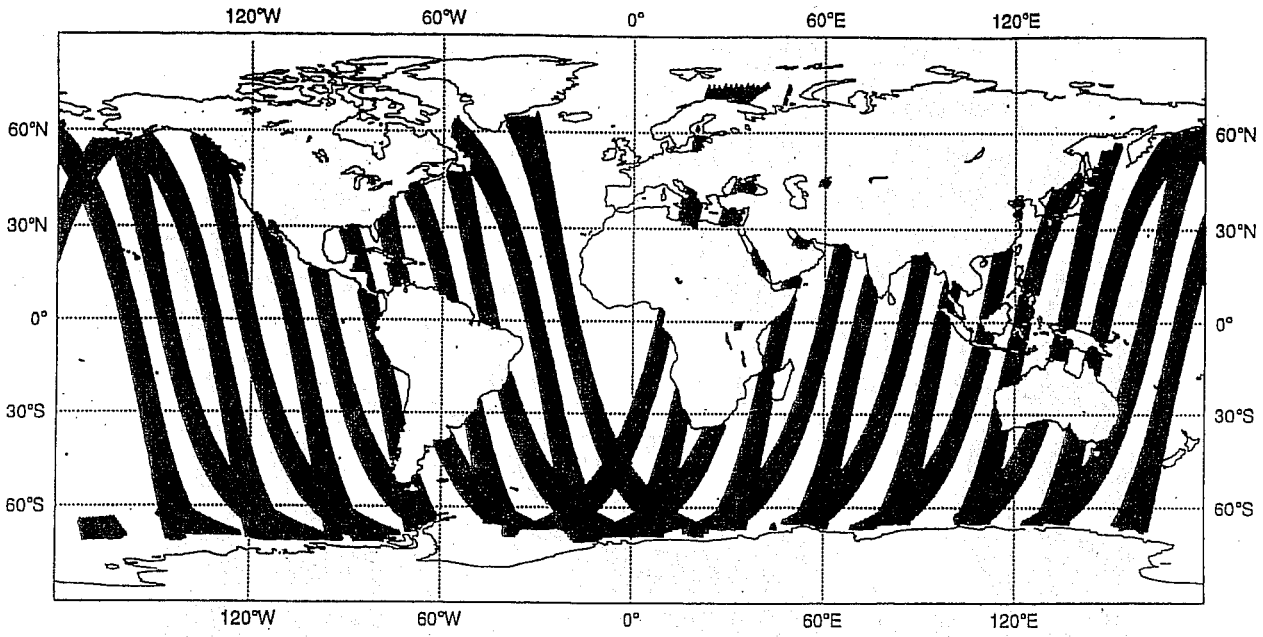

Figure 4 Anticipated ASCAT data coverage in 12 hours.

SeaWinds, which was the next scatterometer to become operational, is realised on a dedicated polar satellite, QuikSCAT, launched in June 1999. QuikSCAT is the first scanning scatterometer featuring a pencil beam radar. A scanning scatterometer may accomodate a broad swath. However, a disadvantage of such a concept is that at the extreme ends of the swath, the earth surface is only illuminated from a single azimuth direction, Moreover, in the middle of the swath, at the so-called subsatellite track, the ocean is only illuminated from two exactly opposite directions. The limited azimuth sampling means that wind direction can only be poorly resolved at these locations. Fortunately, the total QuikSCAT swath width of 1800 km guarantees that the full wind vector can be determined accurately over a large range across-the swath.

The record-fast QuikSCAT programme was planned after the dramatic loss of NSCAT, in order to fill the gap between the ADEOS-I and ADEOS-II missions. ADEOS-II will carry a scatterometer very similar to QuikSCAT, called SeaWinds, and is planned to deliver data in early 2002. SeaWinds on QuikSCAT and on ADEOS-II in late 2001 may provide a bridge between the ERS and METOP missions in case that the ERS-2 scatterometer instrument fails and then provide a continuous scatterometer data availability to suit the well-established meteorological user community.

SASS, NSCAT, QuikSCAT, and SeaWinds use a microwave wavelength of 2.1 cm (14.6 GHz frequency; denoted Ku-band). This frequency is affected by atmospheric attenuation due to cloud liquid water and rain. Furthermore, rain droplets hitting the ocean surface distort the gravity-capillary waves, and may complicate the backscatter-wind relationship. Latter effects become substantially smaller for a higher wavelength. To avoid such effects and focus on reliable wind data below cloud, the ESA scatterometers on board the ERS-1 and ERS-2 satellites, and the ASCAT scatterometer planned on the European METOP satellite series use a wavelength of 5.7 cm (5.3 GHz frequency, denoted C-band).

2.2 ERS SCATTEROMETERS AND ASCAT

The first ESA remote sensing satellite, ERS-1, was launched on 17 July 1991 into a polar orbit of 800 km height. In 1995 the ERS-1 follow-on, ERS-2, was launched. The ERS-1 and ERS-2 scatterometers, which are identical and denoted SCAT here, each have three antennae, that

illuminate the ocean surface from three different azimuth directions, as shown in Figure 7. A point on the ocean surface will first be hit by the fore beam, then by the mid beam and at last by the aft beam. *Stoffelen and Anderson* (1997) have shown that this measurement geometry generally results in two opposite wind vector solutions. In *Stoffelen and Anderson* (1998) it is discussed how a unique wind vector solution may be selected from the two optional ones. *Stoffelen and Anderson* (1997) describe the estimation of a backscatter-wind relationship for the wavelength used by SCAT. The SCAT wind product has a high quality and shows small scale meteorological structures, as shown in figure 3.

A limitation of the SCAT is its coverage. In contrast to the NASA Ku-band scatterometers, SCAT only views at one side of the subsatellite track. Moreover, the microwave source is shared with a SAR instrument, so that the operation of SCAT is often not possible in meteorologically interesting regions (e.g., in the Norwegian Sea). Tandem ERS-1 and ERS-2 SCAT numerical weather prediction impact experiments by ECMWF (*Le Meur*, 1997) and KNMI (*Stoffelen*, 1997) have shown that two scatterometers have more than twice the value of one.

The ASCAT (advanced) scatterometer due on METOP, which is planned for launch in 2003, will use the same radar wavelength as SCAT, but will be double sided and have a dedicated microwave source. Figure 4 shows the coverage that would be obtained by ASCAT over a period of 12 hours. The interpretation of ASCAT will thus benefit much from the knowledge gained during the ERS missions.

Because of the fortuitous antenna configuration of the ERS scatterometers, a practical and straightforward solution for the inversion problem exists (*Stoffelen*, 1998). In case of NSCAT, the antenna geometry is less ideal, but this is compensated by the use of a fourth measurement in horizontal polarisation for the mid beam; ERS uses only vertical polarisation measurements. The SeaWinds instrument, which in comparison with the NSCAT fan-beam scatterometer has the following advantages: higher signal-to-noise ratio, smaller in size, and superior coverage. On the other hand, the SeaWinds scanning scatterometer concept poses new challenges to an effective extraction of wind information. SeaWinds has an antenna illumination pattern that is dependent on node number or cross-track location (WVC), due to its circular scans on the ocean. The skill of the wind retrieval algorithm and subsequent QC depends very much on the number of measurements and their polarization (horizontal HH or vertical VV) and "azimuth diversity", where azimuth diversity is defined as the spread of the azimuth looks among the measurements in the WVC. The nadir region has fore and aft looks of both beams (HH and VV) nearly 180° apart. At the edges of the swath the outer VV beam fore and aft looks are nearly in the same direction and no inner HH beam information is available. In both areas, the skill of the wind retrieval algorithm is decreased with respect to the rest of the swath (called the sweet zone) where there are four measurements (fore-HH, fore-VV, aft-HH and aft-VV) with enough azimuth diversity. In this paper, we will mainly focus on this sweet zone, 1100 km wide.

3 GEOPHYSICAL MODEL FUNCTION

In scatterometry a microwave beam is emitted to the ocean surface under an angle. This radiation, with a wavelength of some centimeters, will be scattered and reflected on the rough ocean surface and a small part of the power emitted will be returned to the detector of the scatterometer instrument. A scatterometer has a footprint of several tens of kilometers in diameter with generally a large number of scattering elements in it. For such a distributed target one may define a dimensionless microwave cross section per unit surface, often denoted "Normalized Radar Cross Section" or NRCS and by convention written as σ^0. σ^0 is generally expressed in dB, i.e., as the value of $10\log(\sigma^0)$. The backscattered power turns out to be well correlated with the ocean near-surface wind conditions, and empirical relationships exist that describe this correlation (see, e.g., *Stoffelen*, 1998; or *Wentz*, 1984). Here, we first discuss the physical principles.

3.1 PHYSICS

Several attempts have been made to provide a theoretical framework in which all aspects of scatterometry are tackled, e.g., *Donelan and Pierson* (1987) or *Snoeij et al.* (1992). Below we highlight some main aspects.

The relevant physical phenomenon that is important for the working of the scatterometer is the presence of the so-called gravity-capillary waves on the water surface. Gravity-capillary waves have a wavelength of some centimeters and respond almost instantaneously to the strength of the local wind (*Plant*, 1982). Resonant microwave scattering strongly depends on the amplitude of the gravity-capillary waves. Furthermore, these waves tend to align perpendicular to the local wind direction and thus the ocean radar return is wind direction dependent and thus anisotropic. Several approximations exist that theoretically try to describe the interaction of e.m. waves with the ocean surface (see, e.g., *Snoeij et al.*, 1992). However, for laboratory experiments in a wave tank these different models show a dispersion of several dB, which is large compared to the accuracy of the ERS scatterometer of 0.2 dB.

The topography of a rough ocean surface is much more complicated and dynamic than the relatively simple wave states that are usually generated in laboratory experiments (e.g. *Mastenbroek*, 1996), which is further complicating a useful description of the interaction of a microwave beam with such an ocean surface. Furthermore, the local interaction theories need to be extended in order to provide a useful theory over a scatterometer footprint and take into account the sea state spatial variability (e.g., *Stoffelen*, 1998; *Donelan et al*, 2000).

There is a relationship between the energy density of the gravity-capillary waves and the so-called surface shear stress (momentum flux), denoted τ, which is a measure of the impact the wind has on the ocean surface. Wind shear stress is not a practical variable to use for calibration or validation, since its observation is complicated and measurements of this quantity are not widely available. Wind measurements at a reference height of 10 m, which is in the so-called surface layer, are widely available. However, the relationship between surface stress and wind at 10 m, is not without uncertainty either and differences of 20 % occur easily (*Stoffelen*, 1998).

3.2 EMPIRICS

The empirical approach followed for ERS is to relate σ^0 to the wind at 10 meter height above the ocean surface, simply because such measurements are widely available for validation. This means that any effect that relates to the mean wind vector at 10 meter height is incorporated in the backscatter-to-wind relationship. As such, since air stability, the appearance of surface slicks, and the amplitude of gravity or longer ocean waves, depend to some degree on the strength of the wind, these effects will, to the same degree, be fitted by a backscatter-to-wind transfer function. *Stoffelen* (1998) further describes these effects. *Stoffelen and Anderson* (1998) describe the ins and outs of emperical fitting of the GMF.

4 BACKSCATTER DOMAIN

It is of great value to visualise sets of measured σ^0 observations for (*Stoffelen and Anderson*, 1997a)

- checking the validity of the geophysical model function (GMF) that is used in the inversion;
- a visual check of the data to characterise noise and to identify outliers (QC);
- depicting the geometry of the inversion problem; and
- depicting the non-linear nature of the scatterometer data assimilation problem.

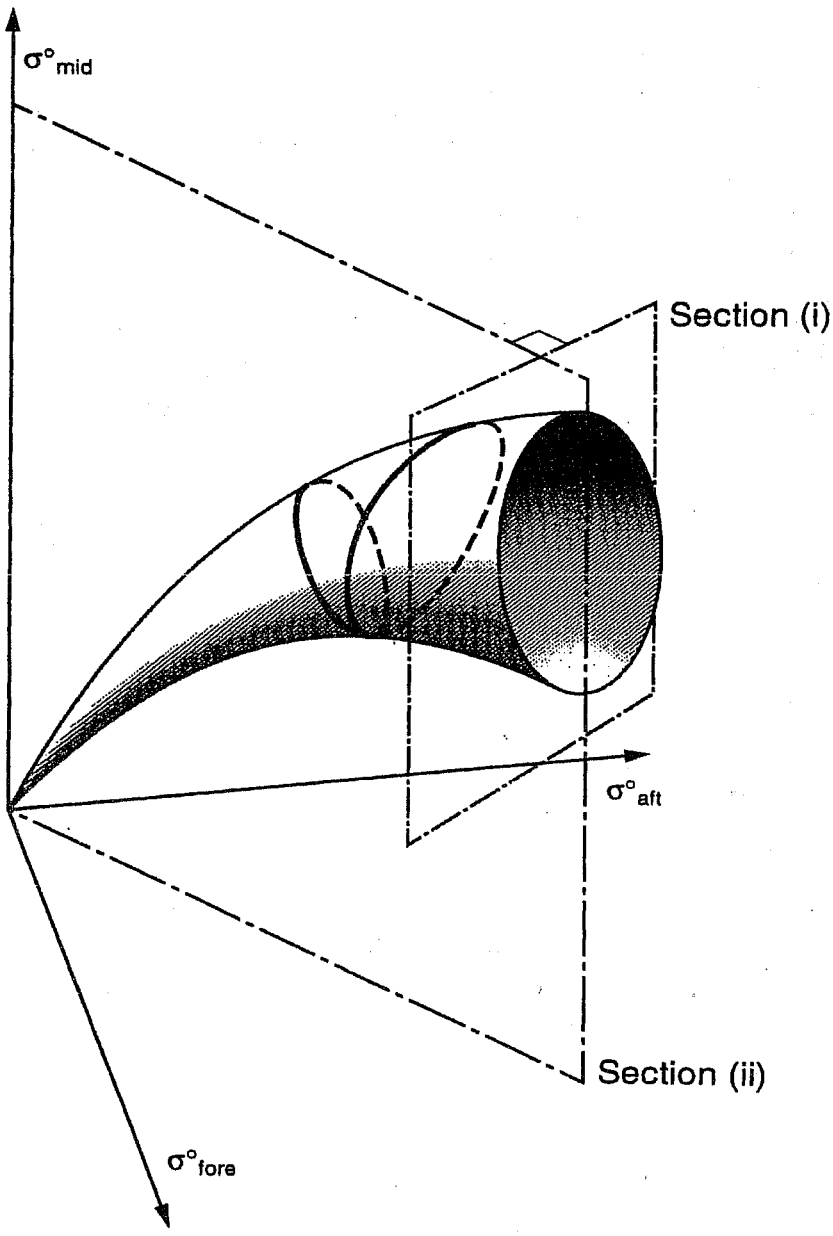

Figure 5: Sketch of the cone surface in the ERS scatterometer measurement space spanned by the fore, mid, and aft backscatter measurements at each node. Sections across the cone (i) and along the cone (ii) are useful to visualise the properties of the cone. The thick solid and dashed line gives the modualation of the backscatter triplet with varying wind direction for a fixed wind speed, depicting the double sheath of the cone resulting in a wind direction ambiguity.

The most fruitful visualisation of the backscatter measurement (phase) space that was applied for ERS scatterometer data was to make a selection of $\sigma^0_{\text{fore}} + \sigma^0_{aft} \approx$ constant, and to plot $\sigma^0_{\text{fore}} - \sigma^0_{aft}$ against σ^0_{mid}. Why this is fruitful can be understood by elaborating on a rough expression of the GMF

$$\sigma^0(V,\phi;\theta,\alpha,p) = A_0 + A_1\cos(\phi-\alpha) + A_2\cos(2\phi-2\alpha) \tag{1}$$

where V is wind speed, ϕ wind direction with respect to the mid beam pointing direction, p the polarisation, θ the incidence angle, and α the azimuth look direction with respect to the mid beam pointing direction; $A_i = A_i(V,\theta,p)$, and, particularly for V-polarisation, $A_1 << A_2$. If, as for the ERS scatterometers, we further realise $\alpha_{\text{fore}} = -\alpha_{aft}$ we find

$$\begin{aligned} \sigma^0_{\text{fore}} + \sigma^0_{aft} &= 2A_0 + 2A_2\cos 2\alpha\cos 2\phi \\ \sigma^0_{\text{fore}} - \sigma^0_{aft} &= \quad 2A_2\sin 2\alpha\sin 2\phi \end{aligned} \tag{2}$$

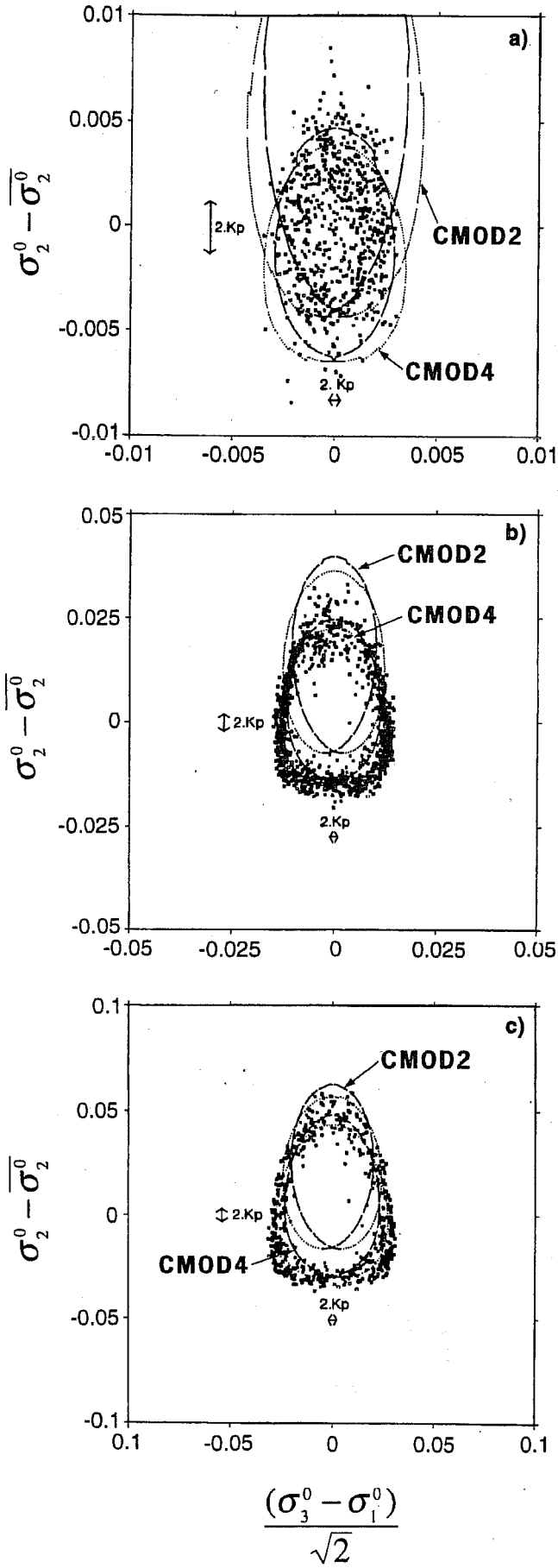

Figure 6: Cone cross section (see figure 5) for node 11 with 5% thickness for a wind speed of about (a) 4 m/s, (b) 8 m/s, and (c) 12 m/s. The scale of the plots vary, but is the same for abscissa and ordinate. 2Kp indicates a measure of the expected instrumental noise. CMOD2 is the pre-launch GMF, whereas CMOD4 is the GMF currently used and recommended by ESA.

where α is really α_{fore}. Since for ERS $\alpha_{\text{fore}} = 45^o$ and $\alpha_{mid} = 0^o$ we find the three independent coordinates

$$\begin{aligned} \sigma^0_{\text{fore}} + \sigma^0_{aft} &= 2A_0 \\ \sigma^0_{\text{fore}} - \sigma^0_{aft} &= 2A_2 \sin 2\phi \\ \sigma^0_{\text{mid}} &= A^m_0 + A^m{}_2 \cos 2\phi \end{aligned} \tag{3}$$

This means that taking a cross-section $\sigma^0_{\text{fore}} + \sigma^0_{aft}$ = constant, comes down to keeping the wind speed (almost) constant. Therefore, in such a cross-section where the axes are determined by the other two coordinates, one can easily draw the GMF curve that (almost) describes a double elliptical shape for varying ϕ, together with the measurement points, and hence simply check the validity of the GMF or the relative calibration of the fore and aft beams. Note that A_0 and A_2 increase with increasing wind speed such that in three dimensions the GMF describes a cone-like surface (*Stoffelen*, 1998; see figure 5).

Figure 6 shows a cross-section through the cone. The noise properties of the cone can be seen, as well as some points close to the centre of the cone. These points are often close to a front or low and likely due to non-linear effects or anomalous sea state conditions such as a confused sea state. It may be clear that it will be difficult to assign a unique point on the cone to these points, in other words, we canot retrieve a meaningfull wind vector. As such, these points are rejected by a test of their "distance to the cone" or normalised inversion residual in 1 or 2% of ERS cases.

Distances to the cone are generally compatible with the expected instrument noise characteristics and the geophysical noise due to footprint collocation mismatches (*Figa and Stoffelen*, 1999). Recently, however, it has been discovered that the triplets remain inside or outside the cone surface, depending on a spatially smooth geophysical variable. Preliminary checks indicate that wind spatial variability or convection is the likely cause. A simple explanation is that the varying wind in a footprint causes the mean triplet backscatter to fall into the cone (see also figure 8). More work is needed to further quantify this effect.

The NASA scatterometer, NSCAT, on board the Japanese ADEOS-I was tested in a similar way. Here, a complication lies in the fact that in addition to vertical polarisation, horizontal polarisation is used on the mid fan beam, where no longer $A_i << A_2$ applies. The second complication is that the mid beam is at $\alpha_{mid} = 25^o$. Nevertheless, *Figa and Stoffelen* (1999) describe a transformation that separates the wind speed and harmonic wind direction dependence. *Stoffelen, Voorrips, and de Vries* (2000) describe the usefullness of the concept of measurement space for SeaWinds. It turns out that the concept of "distance to the cone" is of eminent importance for the QC of NSCAT and SeaWinds. The contamination by rain is the main reason, since at Ku-band retrieved scatterometer winds are detrimentally affected in case of rain. *Figa and Stoffelen* (2000) and *Portabella and stoffelen* (2000) describe a successful QC method based on "distance to the cone" to include rejection of rain-contaminated points in case of respectively NSCAT and SeaWinds. Figure 1 provides an example of this. SeaWinds on ADEOS-II may profit from AMSR for rain elimination (*Boukabara*, 2000), when all parts of the swath may be checked for rain.

Another application of the backscatter domain is its use for the instanteneous discrimination of points over ice from wind points. This is developed in the context of the Ocean and Sea Ice Satelite Application Facility at KNMI in order to improve the real-time capability of wind retrieval close to the ice edge.

5 WIND VALIDATION AND CALIBRATION

The cone surface is spanned by two geophysical parameters as described by the GMF. Empirical wind tuning thus comes down to mapping these two parameters to the wind at 10 m height, i.e., wind calibration.

5.1 TRIPLE COLLOCATION

In chapter IV *Stoffelen* (1998) emphasizes that what is most comonly done to validate meteorological variables is in fact imprecise. It is common practise to compare two noisy collocated observations with different random error characteristics or spatial and temporal representation with each other. Without precise knowlege of the errors it is in fact not possible to calibrate one data set against the other. However, *Stoffelen* (1998) shows that with three collocated observation sets, it is possible to calibrate two of the data sets against the third and reference observations. For two different data sets and at the spatial representation of the NWP models he found the results in table 1.

	Along-Track Component		**Across-track Comonent**	
In situ/ NWP model	NOAA/ NCEP	North Sea'94/ ECMWF	NOAA/ NCEP	North Sea'94/ ECMWF
Number	1465	3762	1465	3732
Variability [ms^{-1}]	4.68	6.70	5.24	6.53
In situ [ms^{-1}]	2.02	2.65	1.89	2.58
Scatterometer [ms^{-1}]	1.89	1.86	1.62	1.65
Model [ms^{-1}]	1.11	0.95	0.97	0.86

Table 1 Triple collocation results of the random observation error from in situ data, ERS scatterometer, and NWP model data. NOAA/NCEP includes NOAA buoy winds corrected to 10-m height and NCEP model winds, whereas the right data set includes bouys and platforms in the North Sea without height correction and the ECMWF model winds.

It may be surprising that the NWP models are so accurate compared to the scatterometer and the buoys. However, note that the spatial variability resolved by the scatterometer or the buoy, but not by the NWP model is treated as random scatterometer or buoy observation error, as is common practise. From the table it is clear that some common statistics in fact could be quite misleading:

- *Stoffelen* (1998) shows that the mean difference of NWP model speed and *in situ* speed as a function of the *in situ* speed can go up to 1 m/s (pseudo bias) because of the nonlinear transformation of these random errors to wind speed.
- if an unweighted regression is done then too much weight would be put on the in situ observations and the NWP calibration coefficient would be wrong by about 5%.

Triple collocation avoids these types of problem. The difference in NOAA and North Sea buoy random error is very likely the effect of height correction.

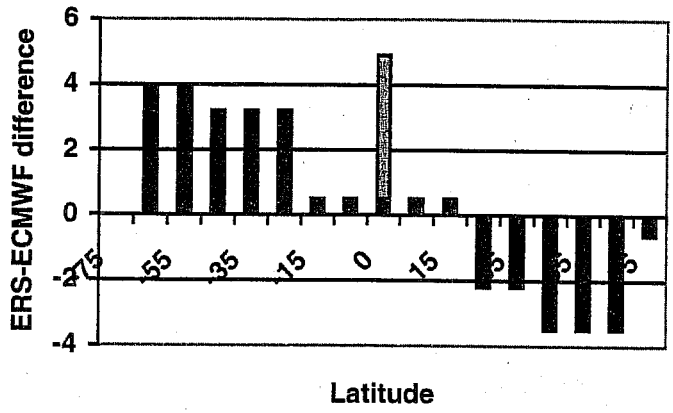

Figure 7 Wind direction difference between ERS scatterometer and ECMWF model (in November 1994).. An unexplained hemispheric effect and an equator bias stand out. Similar effects are reported for NSCAT and SeaWinds.

5.2 WIND DIRECTION AMBIGUITY

One can validate the inverted wind direction against a reference wind direction, such as from NWP models or buoys, by taking the closest to the reference, and computing the RMS difference. However, it is clear that the more ambiguous solutions are provided by the inversion, the *smaller* the RMS will be, because the chance that one of the solutions will be close to the wind reference will increase. In the limit of an infinite amount of observations, the RMS will even be zero, while the information content of the set of solutions in reality *decreases* with an increasing number of solutions, because there is no a priori way to say which of the solutiuons is the correct one. To avoid this problem, one can validate the selected (by ambiguity removal, AR) or the rank-1 solutions, but since both rank-1 skill and AR skill are not perfect, these approaches reveal a pessimistic view on the inherent information content of the scatterometer regarding wind direction. One may expect that the rank-1 skill and the AR skill generally decrease with an increasing number of solutions. To aid in the validation of wind direction, *Stoffelen, Voorrips, and de Vries* (2000) define a "normalised" RMS (NRMS) difference, which reflects in a fair way the quality of the closest solution. This NRMS contains a normalisation factor which is equal to the expected value in the case that there is no skill in the system, thereby taking into account the inherent ambiguous nature of these observations.

6 OBSERVATION SMOOTHING

SeaWinds data are nominally provided with a sampling of 25 km, whereas most NWP models use observations at at least a 100-km density. The small-scale structures observed by a scatterometer cannot be fitted well by the relatively broad spatial structure functions, and statistical noise in the analyses results. For many observing systems data thinning procedures are in use (see e.g., *Rohn et al*, 1999; *Anderson et al*, 1999; *Leidner and Isaksen*, 2000, *McNally*, this issue). The size of the spatial structure functions used in meteorological analysis for spatial extrapolation of the observed variables is mainly determined by the poor observation of the upper air flow (*ESA*, 1999). One could

1. thin the observations;
2. group the observations;
3. average the measurements; or
4. average the satellite product.

in order to arrive at a smoother representation of the observations. The first method is useful when the observation errors are spatially correlated, or when the errors are spatially heterogeneous and the thinning can be used to select the high-quality data. By observation grouping I mean the assignment of the mean location to a group of nearby observations. It has the advantage with respect to thinning that all information in the observations is kept. *De Vries and Stoffelen* (2000) adopted this method in an ERS scatterometer 2D-VAR, whereby the ambiguity patterns of all individual 50-km

ERS scatterometer wind observations are kept, but still a spatial averaging effect is achieved in order to reduce phase errors in the 2D-VAR analysis. Approach 4 has been used by *Stoffelen and Beukering* (1998) and indeed they showed that averaged winds compare better to the HIRLAM (2000) first guess than thinned data. However, for scatterometer data, in order to reduce systematic wind retrieval errors, it appears better to reduce noise and average σ^0 to lower resolution before the non-linear wind retrieval process.

The above problem of numerically analysing small-scale weather patterns provides an important motivation to present scatterometer wind data to operational meteorologists for nowcasting and short-range forecasting purposes (see e.g. figure 3). However, still appropriate quality of the retrieved winds and ambiguity removal has to be achieved in order to present a reliable product. This is not generally achieved in the 25-km near-real time QuikSCAT BUFR product. In order to improve quality and reliability we investigate the effect of spatial smoothing of the backscatter data (*Stoffelen, Voorrips, and de Vries*, 2000). Non-linear effects need to be considered in the processing of the averaged data as depicted in figure 8.

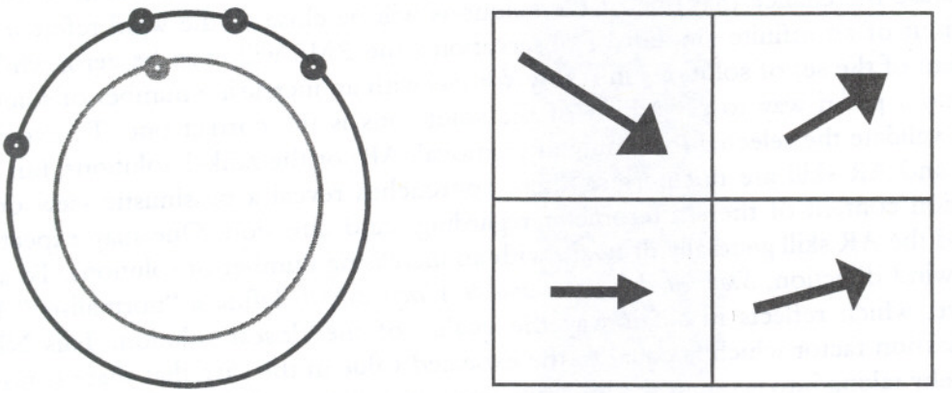

7 DIRECT VERSUS INDIRECT ASSIMILATION

Lorenc (1988) provides a detailed and comprehensive description of the problem of data assimilation. He derives the equations for "optimal" nonlinear objective analysis that form the basis of many current variational data assimilation schemes, using maximum probability as the major constraint. *Stoffelen* (1998a; chapter VI) describes the problem of the analysis of variables that are related in a non-linear way to the NWP model variables, such as scatterometer backscatter measurements. He suggests that normal distributed noise can introduce systematic biases when constraining a minimum variance or maximum probability solution, if the relationship that is used in the analysis between observed and model variable is not linear. If the goal in data assimilation is to achieve an unbiased estimate of the model state then the term "optimal" for a maximum probability solution in combination with the phrase nonlinear appears misleading.

This is illustrated in figure 9. Suppose x denotes the model state, and $f(x)$ is the nonlinear observation operator for the observation y, then Gaussian uncertainty in x is projected by $f(x)$ into a skew and multi-modal distribution in y. The maximum probability solution in y of the projected solution does not provide an unbiased solution, if not ambiguous.

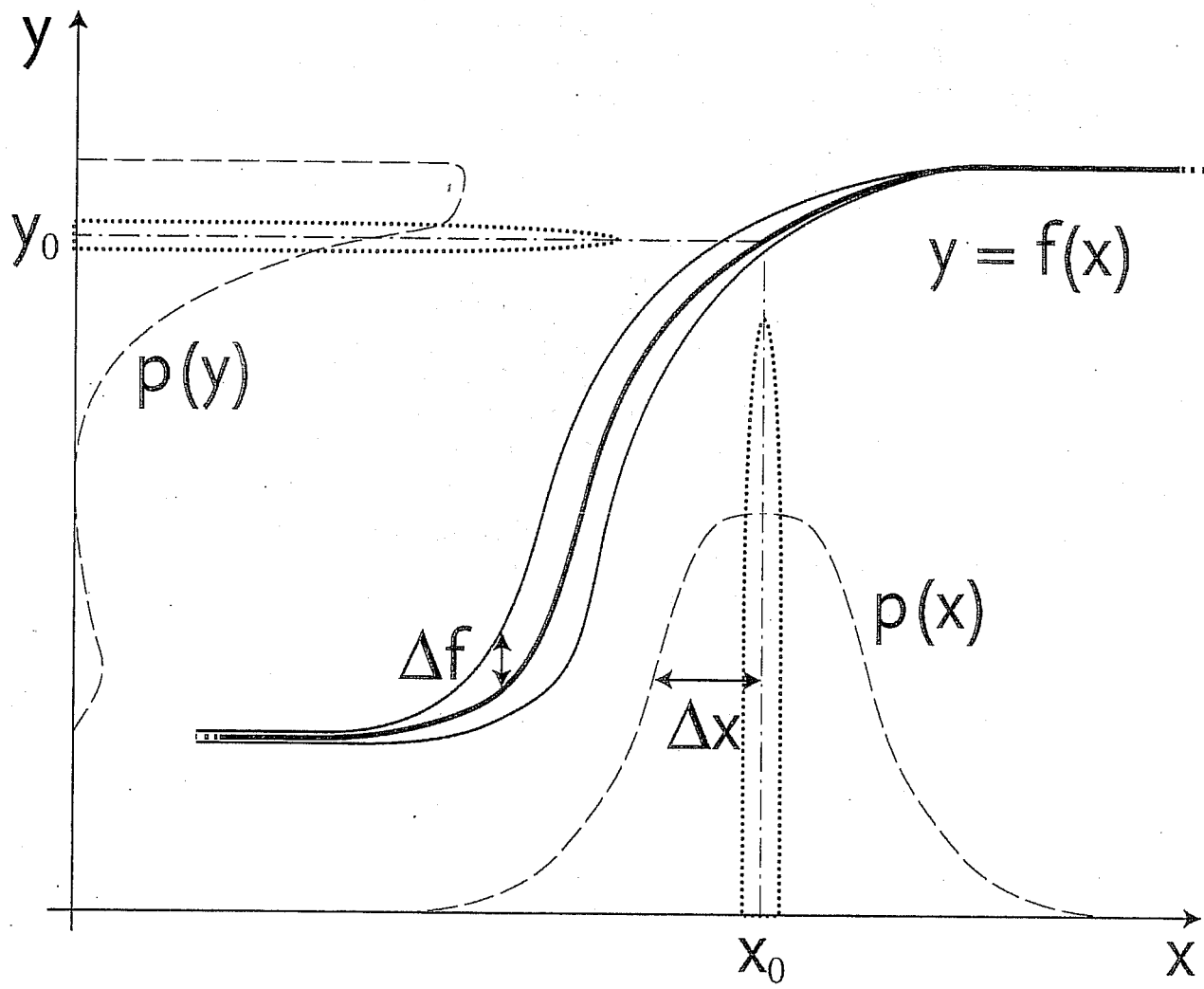

Figure 9: Non-linear transformation of a normal distribution p(x) *with mean* x_0 *and of width* Δx *to the skew and multi-peaked distribution* p(y) *through an equation f with uncertainty* Δf. *The projection of the median* x_0 *of* p(x) *to the median* y_0 *of* p(y) *is shown by the dash-dotted line. For* p(y) *the median, mwean, most likely, and minimum variance values of* y *are all different. The dotted lines show the quasi-linear projection of a narrow error distribution from* y *to* x.

As the most practical solution for the assimilation of scatterometer data, *Stoffelen* (1998) suggests to assimilate retrieved scatterometer winds. This approach is further pursued for SeaWinds scatterometer observations (*Stoffelen, Voorrips, and de Vries*, 2000). Scatterometer winds are generally determined accurately from a backscatter multiplet, since backscatter noise is small for all scatterometer systems. Backscatter-only noise results in a wind vector uncertainty of only about 0.5 m/s after the non-linear inversion. In analogy with the discussion in the previous paragraph, in figure 9 this is depicted by a narrow distribution at x_o. The corresponding distribution in y is then also a narrow distribution at $y = y_o$. As such, no biases appear. However, the interpretation of a radar backscatter measurement, that is most directly related to the anisotropic roughness of the ocean topography on the cm-scale, as a wind at 10m height introduces a much larger uncertainty that can be well modelled by a normal wind component error distribution (*Stoffelen*, 1998b). As a result, wind vector measurements from a scatterometer have an estimated accuracy of about 2 m/s. The larger and close to normal distributed uncertainty in the wind domain makes the assimilation of retrieved winds more attractive than the direct assimilation of backscatter measurements.

Moreover, in the direct assimilation of backscatter observations, one would transform the first guess or control variable (wind) errors in a non-linear way to the backscatter space, resulting in a biased and skew error distribution in this space (as in figure 9). The first guess vector error is about 1.5 m/s (see table 1). The precise form of the error distribution in σ^0 would depend on wind speed, wind direction, and view configuration. As said above, the maximum probability in a skew distribution does generally not overlap with the mean of the distribution, nor has the maximum symmetric properties. In line with this, the assumptions made to derive a quadratic cost function in variational data assimilation (2D-VAR, 3D-Var, 4D-Var) that

1. a priori all states of the control variable are equally likely; and that
2. the deviation between true state and background can be described by a Gaussian distribution;

are invalid in the backscatter space. The optimal observation cost function and observation operator is not a priori clear in such a case and requires considerable thought (*Stoffelen*, 1998; chapters V and VI). By assimilating retrieved winds this problem disappears, since the above assumptions do hold by approximation in this domain.

NSCAT and SeaWinds use horizontal and vertical polarisation measurements, whereas ERS or ASCAT are solely based on vertical polarisation. This in combination with a varying measurement geometry results in a different wind direction ambiguity structure than for ERS or ASCAT. As a result, more wind vector solutions are present, but with varying skill.

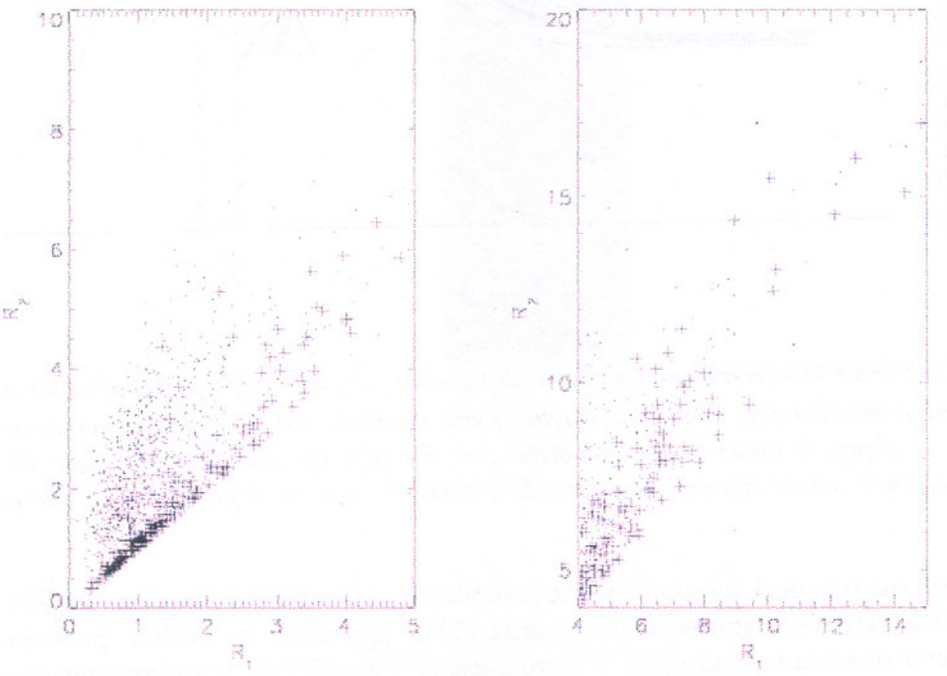

Figure 10: Scatter plot of first rank normalised inversion residual R_1 against second rank solution residual R_2 only for cases with two solutions. Dots indicate pairs where the first rank is the one closest to the NWP wind velocity; plusses are pairs where the second rank is selected. The left panel highlights only the lower range residuals of a total of 1,500 pairs, whereas the right panel only shows higher range pairs of a total of 15,000 pairs. For $R_1 < 3$ the first rank is almost always selected, unless $R_1 \approx R_2$. For higher R_1 either rank may be selected, indicating less predictive skill in the residual. Note however that all points in the right panel are screened by our QC. As such, SeaWinds ranking information appears to be an excellent predictor.

7.1 A GENERAL SCATTEROMETER ASSIMILATION APPROACH

The ERS scatterometer cost function may be generalised to be able to cope with all scatterometer data. All scatterometer data can be characterised by multiple wind vector ambiguities that each have different probability and accuracy. A procedure is described here that estimates this probability and accuracy and as such provides the input for a general scatterometer cost function.

Generally data assimilation systems constrain to a background or first guess field and to observations (e.g., *Lorenc*, 1988; and *Courtier et al*, 1998) in a minimisation problem of the objective function

$$J = J_b + J_o \tag{4}$$

where J_o is the observation cost function and J_b the background field cost term.

The observation term consists of a contribution from each observation and is related to the probability of a meteorological state, given the measurements. For scatterometer data we write

$$J_o^{SCAT} = -2\ln\{p(\sigma_O^0 \mid \mathbf{v})\} \tag{5}$$

where, for a set of scatterometer data, $\sigma^0{}_O$ we may write for the probability of the surface wind $\boldsymbol{V}$

$$p(\sigma_O^0 \mid \mathbf{v}) = \sum_{i=1}^{N} w\{p_i^p\, p_i(R_i)\} N(\mathbf{v}_i, \boldsymbol{\varepsilon}_i) \tag{6}$$

where p_i^p is the prior probability of a solution i, $i \in [1, N]$, i.e., without knowledge of the "distance to the cone", R. It is solely dependent on the wind direction sector that a solution represents and only relevant in case of more than two solutions, i.e., $N > 2$. For $N > 2$, the prior probability p_i^p just depends on the azimuths of the solutions (*Figa and Stoffelen*, 2000) and if we define wind direction sector boundaries $\phi_i^B = (\phi_{i-1} + \phi_i)/2$ (with $\phi_0 = \phi_N$) we can write

$$p_i^p = \frac{\phi^B{}_{i+1} - \phi_i^B}{2\pi} \tag{7}$$

$p_i(R_i)$ is the probability of a solution based on the normalised residual of the solution i. $N(\mathbf{v}_i, \boldsymbol{\varepsilon}_i)$ is a normal distribution with maximum at the wind solution $\mathbf{v}_i$ and error width $\boldsymbol{\varepsilon}_i$. For ERS scatterometer data (*Stoffelen*, 1998) the values $N = 2$, $p_i^p = 0.5$, $p_i(Rn_i) = 1$, $w = 0.5$, and $\boldsymbol{\varepsilon}_i = (\varepsilon_U, \varepsilon_V)$ with $\varepsilon_U = \varepsilon_V =$ 1.5 m/s are used.

We discussed before the concept of measurement (phase) space. In this space a 2D surface, called cone, exists spanned by the two wind vector variables (u,v) or (V, ϕ). R is then denoted "distance-to-the-cone" and is a measure of how well a particular measured triplet fits the wind surface in the measurement space. Thus, a measured backscatter triplet is transformed into three independent variables, i.e., R, u, and v. In the formulation above, the three variables $p(R)$, ε_U, and ε_V determine the quality or information content of these three parameters. It thus appears logical to assume $(\varepsilon_U, \varepsilon_V)$ independent of R, since these represent the independent wind variables.

The generalised methodology presented here may also be adopted for those parts of the swath where the wind vector cannot be fully determined, because of limited azimuth or polarisation coverage, and where the ambiguity pattern can be of greater complexity. However, in these parts of the swath the solution minima may be less well defined than in the sweet zone, because of the wind vector underdeterminacy. In that case, the width of the minimum can be decomposed into two independent wind components, e.g., along the wind vector solution and across, or any other orthogonal set that models the likely anisotropy of the retrieval solution minimum width. $\boldsymbol{\varepsilon}_i$ is then determined by the widths of the retrieved minimum and by the isotropic geophysical interpretation error of about 1.5 m/s in a wind component. Another limitation is that for some parts of the swath

QC may be difficult and assimilation therefore more risky (see section 4 above). AMSR on ADEOS-II is likely to ease this problem.

7.2 *R* DEPENDENCE OF THE COST FUNCTION

In the case of QuikScat, the number of solutions ranges from 1 to 4 (as JPL, we truncate at four in this paper) with R strongly varying from one solution to the next. Since

$$R \approx -2\ln\left\{p\left(\mathbf{v} \mid \sigma_o^0\right)\right\} \tag{8}$$

is a measure of the distance of a measurement from the wind cone (*Stoffelen and Anderson*, 1997a), it seems reasoneable to assume that with increasing R, the probability decreases that a certain solution is the selected solution, i.e., the one closest to the true wind velocity. As a first step we verified that the fraction of selected solutions decrease rapidly with increasing R indicating that R is a good measure of the probability of a solution (*Stoffelen, Voorrips, and de Vries*, 2000).

Figure 10 shows a scatter plot of those cases which have exactly two solutions. It can be seen again that in the left panel rank 1 is the selected one most of the time and rank 2 is only chosen if R_2 is close to R_1. For large residuals, as in the right panel, the difference between R_2 and R_1 is a less good predictor for selection. However, note that $R_1 > 4$ corresponds to cases that we reject by our QC (section 4). *Stoffelen, Voorrips, and de Vries* (2000) determine a relationship between the normalised residual and solution probability that can be used for SeaWinds.

Figures 11 show the effect of incorporating varying solution probability. The contour values used in both panels are identical. In plot 11a it can be seen that the lower probability solution of the two closely spaced wind vector solutions is narrower than in plot 11b, and therefore indeed less likely. Also the minimum for the isolated wind vector solution is deeper and has a larger "region of influence" in figure 11a compared to 11b. Region of influence can be understood as that part of the wind domain where the gradient points away from a particular solution (note the shift of the contour lines around the origin). The region of influence of a particular solution should be proportional to its probability.

7.3 OPTIMAL FORMULATION

Equations (5-6) can be used to formulate a generic cost function for scatterometer data. However, *Stoffelen and Anderson* (1997c) report the following features of this formalism for ERS data in case that V is smaller than ε_s

- Not quadratic in the minumum; and
- No minimum at either of the solutions, but at $V = 0$.

These authors provide an alternative formulation that cures these features

$$J_o^{SCAT} = \left(\frac{\prod_{i=1}^{N} K_i}{\sum_{i=1}^{N} K_i} \right)^{1/P} \tag{9}$$

where they use $P = 4$ and after *Stoffelen and Anderson* (1997c) we redefine

$$K_i = \left[\left(\frac{u - u_i}{\varepsilon_u} \right)^2 + \left(\frac{v - v_i}{\varepsilon_v} \right)^2 - 2\ln P_i \right]^P \tag{10}$$

In case of more than two solutions, such as with NSCAT or SeaWinds, there will be more occasions when two solutions are close together, i.e., $|\mathbf{V}_i - \mathbf{V}_j| < \varepsilon_s$. As such, it becomes more important which formulation to use. Here we will elaborate on this issue. We note that $2 \ln P_{i=S}$ may be added to the righthandside of (9) in order to provide a more common diagnostic.

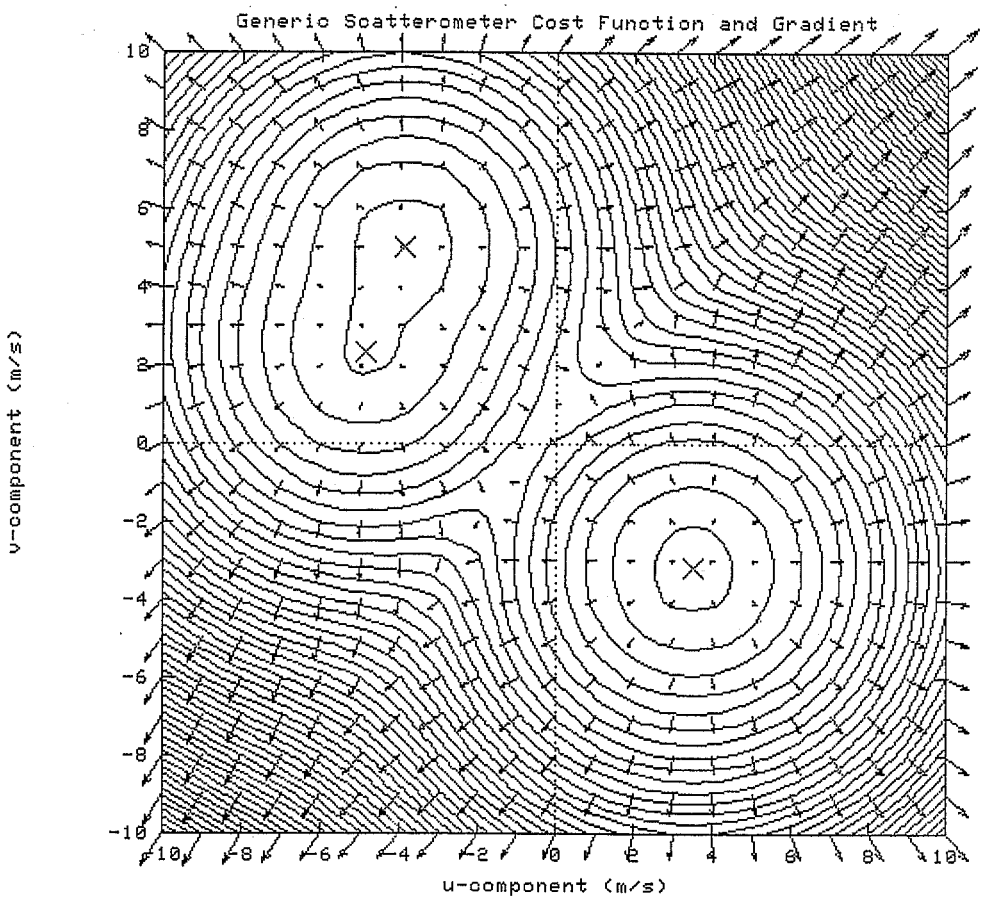

Figure 11a : Plot of the scatterometer cost function with inversion residual and wind direction sector representation appropriately included.

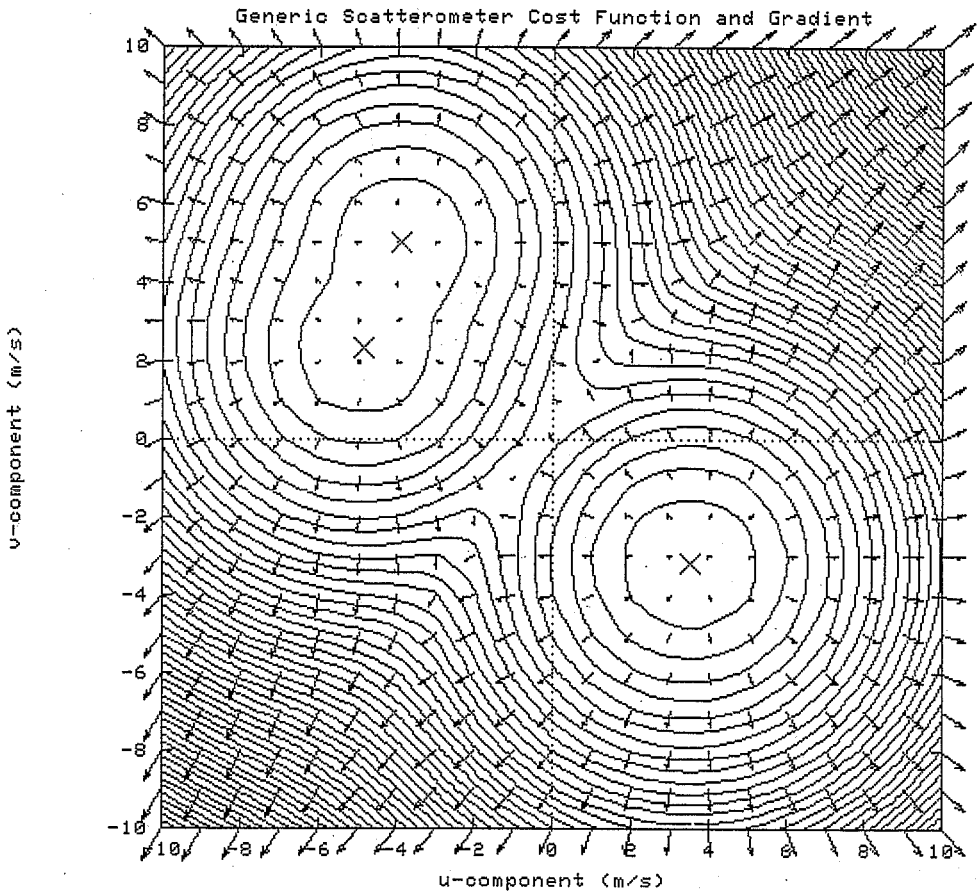

Figure 11b : Plot of the scatterometer cost function and gradient without accounting for direction sector and inversion residual.

Figure 12 shows a simple illustration of the different behaviour of equations (5-6) and (9-10). It represents a case where the scatterometer observes a wind speed of 2 m/s on the ocean surface with 180 degree ambiguity. Using equations (5-6) result in a cost that is minimum at zero wind speed, indicating that this is the most likely wind speed. Physically speaking, this is certainly not right; the ocean capillary-gravity waves will correspond quite well with 2 m/s. If we would systematically use this cost function formulation for these cases, we would get a wind speed that is lower than 2 m/s, i.e., a bias with respect to the scatterometer observation. Apparently, the maximum probability solution that we adopt is biased. *Stoffelen* (1998; chapter 6) shows that in case of non-linear problems, it is not clear what objective results in the best analysis, since a zero bias, minimum variance, or maximum probability constraint can all result in a different answer (see also figure 9).

If we adopt the approach that we want to minimise systematic error in the wind domain, it will be better to have a minimum in the cost function at or very near the wind solutions that are retrieved. In figure 11 it is illustrated that the cost function of equations (9-10) has these properties. In fact, in case one solution is the most likely at a particular wind then it will dominate the cost function, i.e., the formulation acts much like a solution selection algorithm.

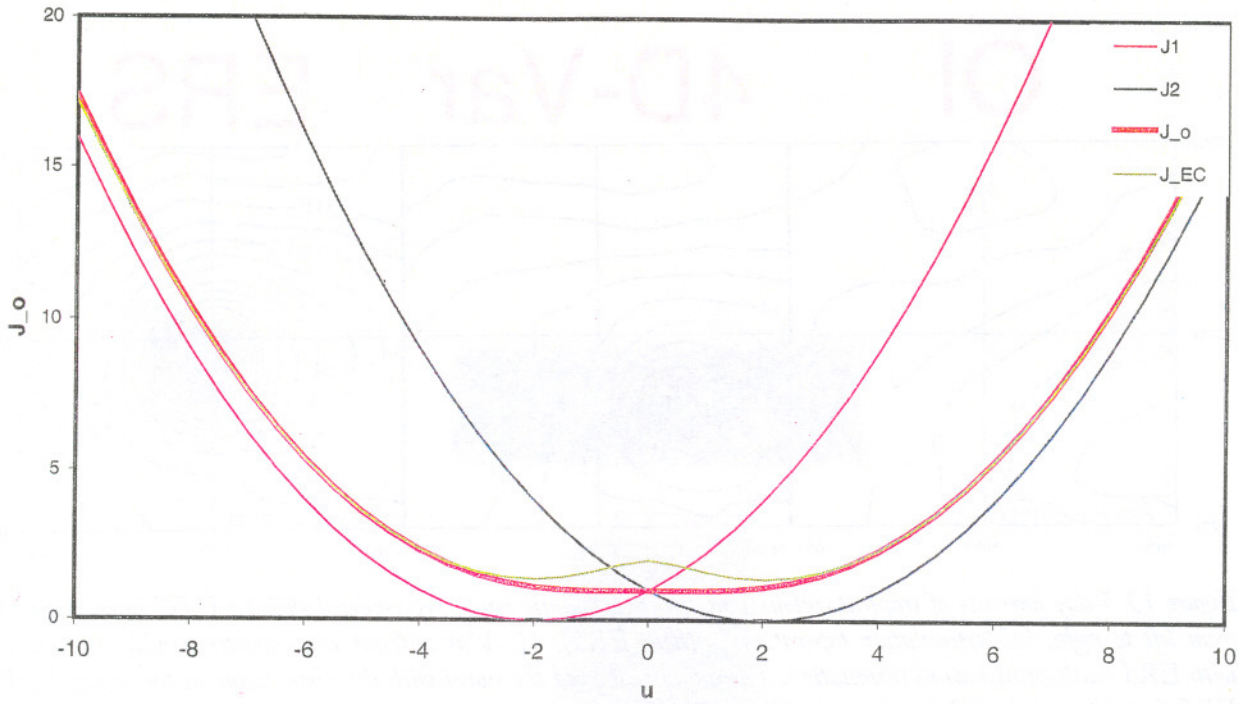

Figure 12: Plot of the generic scatterometer cost function formulation in u for a one-dimensional section along u with solutions $-u_1 = u_2 = \varepsilon_s = 2$ *m/s, and* $P_1 = P_2 = 0.5$. *J1 and J2 present the quadratic contribution of the two solutions respectively, whereas J_o is the total cost using equations (5-8) and J_EC when using the alternative formulation of equations (10-11). In the latter case both solutions are kept as minima.*

Either equations (9-10) or (5-6) can be used to allow variational quality control. In that case, one needs to add a solution with let us say $\varepsilon_s >> 100$ and P_i equal to the expected gross error rate. For the nadir and far swath parts this could be a way to use the winds, but with more stringent QC. This needs to be further explored in the near future. Based on the above discussion we recommend the use of equations (9-10).

8 AMBIGUITY REMOVAL

Ambiguity removal (AR) is the process of selecting the wind vector solution at each observation point in a way that results in a spatially and meteorologically consistent wind field. AR is required when the 1st rank skill is not 100%. For SeaWinds the rank 1 skill is about 80% facilitating the AR process. Thus, despite a substantial fraction of nodes with three or four solutions the AR does not seem complex, since the 2nd, 3rd, and 4th solutions are much less probable. With the cost function as specified above an implicit AR will bedone in 3D-Var or 4D-Var. Moreover, KNMI developed a 2D-VAR for the real-time AR of ERS and SeaWinds scatterometer winds (resp. *de Vries and Stoffelen*, 2000; *Stoffelen, Voorrips, and de Vries*, 2000).

9 OUTLOOK

Scatterometers provide accurate and spatially consistent near-surface wind information. Hardware permitting, there is a continuous series of scatterometers with at times ideal coverage of the ocean surface wind in the coming two decades. In many data assimilation systems, ERS scatterometer observations have proven important for the forecasting of dynamical weather, such as tropical cyclones (*Isaksen and Stoffelen*, 2000). Figure 13 shows a case where 4D-Var improves on the forecast of a tropical cyclone, but where the addition of ERS data provides a much more accurate day-5 forecast of the system. *Isaksen and Stoffelen* (2000) show a systematic improvement in the short- and medium-range forecasting of tropical cyclones when using ERS scatterometer data in 4D-Var. Increased coverage, such as from tandem ERS-1 and ERS-2 measurements, clearly improve the

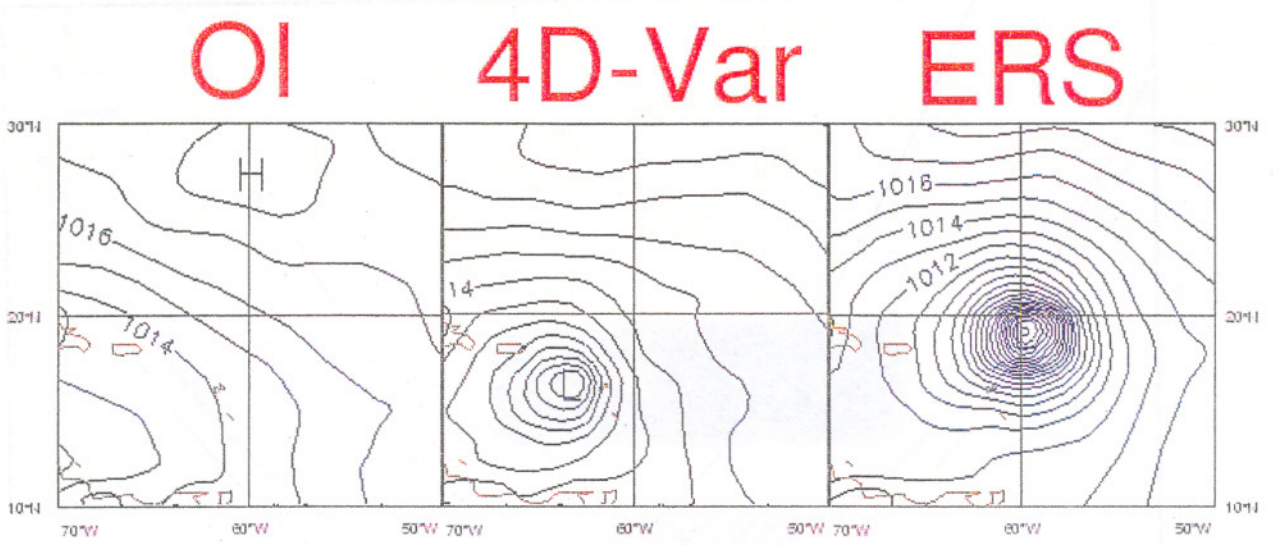

Figure 13 5-day forecasts of tropical cyclone Luis in the Atlantic for 6 September 1995 12 UTC after, respectively from left to right, OI assimilation (operations without ERS), 4D-Var without scatterometer winds, and 4D-Var with ERS scatterometer wind asimilation. The analysis showed the storm with the same vigour as the 5-day 4D-Var ERS forecast, but about 3 degrees to the West of the forecast position.

forecasts of extreme events (e.g., *Stoffelen and Beukering*, 1998; *Le Meur et al*, 1997). Figure 14 shows a figure that emphasises the performance in extreme events. In extreme events short range forecasts tend to differ. Thus, if we plot the verification of both forecasts against the forecast difference, it will become clear which forecast performs best in extreme (dynamical) weather. Obviously, the forecasts are verified against the control analysis as shown in the figure, or even better, against both analyses.

Specific problems in scatterometer data assimilation that we discussed include

- The non-linear relationship between backscatter and wind;
- Lack of physical understanding and the consequent use of empirical modelling;
- Rain contamination in case of Ku-band scatterometers such as NSCAT or SeaWinds;
- Wind vector solution ambiguities;

where we have shown that practical solutions exist to tackle these problems and allow succesful data assimilation.

Since at each node only three or four measurements are used to determine just two variables, it is well possible to visualise the problem of scatterometer data interpretation and assimilation. This is done by making cross-sections through the 3D or 4D measurement (phase) space, where the wind domain spans a 2D surface, called "the cone". It is shown that this cone reveals information on

- The Geophysical Model Function (GMF);
- The noise of the measurements;
- The optimal wind retrieval or inversion process;
- Quality Control (QC) procedures, including rain elimination in case of NSCAT or SeaWinds;
- Backscatter and wind calibration and validation strategy;
- Ice screening procedure; and
- Data assimilation methodology;

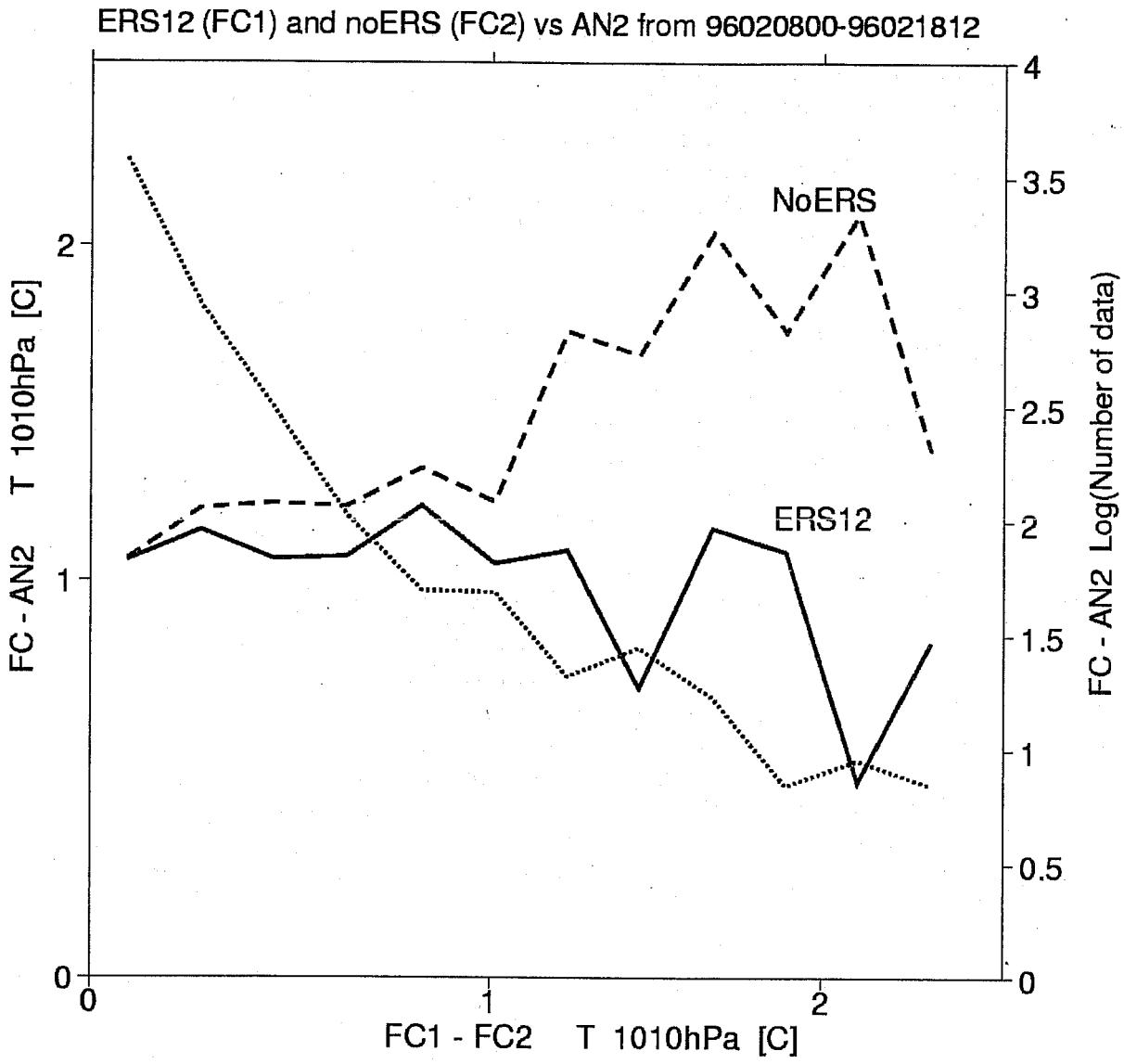

Figure 14 Forecast verification against 2-day forecast difference. Forecast temperature differences are in an area within 1000 km of Amsterdam of a control experiment where no ERS scatterometer data were used and one where tandem ERS-1 and ERS-2 scatterometer data were used. When the forecast difference is large, then the ERS experiment verifies clearly better against the control analyses over the verification period of ten days.

The limited number of variables, and the general overdeterminacy of the wind vector make the scatterometer data interpretation and assimilation problem an excellent playground to study the optimal treatment of measurements that are related in a very non-linear way to the meteorological model state.

Challenges that remain in scatterometry are

- The interpretation of scatterometer observations as ocean wind stress, by investigating the sensitivity of the residual wind error to ocean currents, atmospheric stability, or waves;
- The assimilation of the high spatial resolution of scatterometer winds into NWP models and the achievement of consistent temporal and spatial high-resolution near-surface wind fields; and
- The full exploitation of the more complete coverage of SeaWinds;

Recently, SeaWinds scatterometer measurements from QuikScat have become available. SeaWinds on QuikSCAT provides great coverage over the oceans. Quality monitoring, rain

contamination, wind direction noise characteristics, and wind direction ambiguity selection are now being investigated as a necessary step towards routine and successful use in weather forecasting. It is shown here that the method of data assimilation of ERS scatterometer data can be generalised to include NSCAT and SeaWinds observations. The assimilation of retrieved winds is the most practicable, since retrieved winds are generally unbiased, and because uncertainties in the background winds or control variable, and in the scatterometer retrievals are well expressed as normal errors in the wind domain. However, in the backscatter domain, these error distributions are skew, irregular, and dependent on the wind (direction), due to the non-linear transformation of these errors from the wind to the backscatter domain. As such, the assumptions generally used in meteorological data assimilation do apply if ambiguous scatterometer winds are assimilated, rather then backscatter data directly.

The generic approach for scatterometer wind assimilation uses the normalised inversion residuals ("distance to the cone"} of the solutions and information on the solution pattern to determine the relative probabilities of the wind solutions. The estimated solution probabilities verify very well with the average skill of the ranked solutions. SeaWinds retrievals exhibit an increased number of wind vector solutions with respect to ERS. However, the rank-1 skill is around 80% and therefore ambiguity removal is less demanding than for ERS.

Within the EUMETSAT-funded NWP Satellite Application Facility, SAF, a SeaWinds processing package is being developed that checks, spatially averages, and inverts backscatter data. After these steps a 2D-VAR ambiguity routine is run to investigate the ambiguity removal properties of the cost function and observation operator as described here. Moreover, general scatterometer monitoring software based on mean "distance-to-the-cone" and wind departures will complete the modules under development. After these tests, application in 3D- or 4D-Var data assimilation systems is a straightforward exercise. Following this procedure and based on earlier tandem ERS scatterometer data assimilation experiments, we expect that carefully screened, smoothed, and assimilated SeaWinds scatterometer data from QuikSCAT and ADEOS-II have great potential in state-of-the-art NWP.

10 REFERENCES

Anderson et al, 1999, A Variational data assimilation scheme and its use of meteorological observations, Doctoral dissertation, Dept. of Meteorology, Un. of Stockholm, Sweden, ISBN 91-7153-997-2.

Atlas, R., and R.N. Hoffman, 2000, The Use of Satellite Surface Wind Data to Improve Weather Analysis and Forecasting, in Satellites, Oceanography, and Society, edited by D. Halpern, Elsevier Oceanography Series 63, Elsevier Science, Amsterdam, the Netherlands, ISBN 0-444-50501-6.

Boukabara, S.A., R.N. Hoffman, and C. Grassotti, 2000, Atmospheric Compensation and Heavy Rain Detection for SeaWinds Using AMSR, J. Atmosph. Oceanic Techn., in press.

Courtier, P., et al, 1998, The ECMWF implementation of three dimensional variational assimilation (3D-Var). Part I: Formulation, Quart. J. Royal Meteorol. Soc. 124, 1783-1808.

ESA, 1999, The atmospheric dynamics earth explorer mission, ESA SP1233(4), ESA/ESTEC, Noordwijk, the Netherlands.

Figa, J., A. Stoffelen, 1999, Towards an Improved Ku-band scatterometer wind product, Final report of the EUMETSAT NSCAT Fellowship, KNMI, de Bilt, the Netherlands.

Figa, J., and A. Stoffelen, 2000, On the Assimilation of Ku-Band Scatterometer Winds for Weather Analysis and Forecasting, IEEE-Transactions on Geoscience and Remote Sensing (special issue on Emerging Scatterometer Applications) **38** (4), pp. 1893-1902.

HIRLAM, 2000, http://www.knmi.nl/hirlam.

Isaksen, L., and A. Stoffelen, ERS-Scatterometer Wind Data Impact on ECMWF's Tropical Cyclone Forecasts, IEEE-Transactions on Geoscience and Remote Sensing (special issue on Emerging Scatterometer Applications) **38** (4), pp. 1885-1892.

Jones, Linwood, and David G. Long, 1999, QuikSCAT Radiometric Calibration and Special Brightness Temperature Product, Proceedings from the QuikSCAT cal/val - early science meeting, 2-5 November 1999, JPL, Pasadena, California.

KNMI satellite section web site. http://www.knmi.nl/onderzk/applied/en/sd_index.html

Leidner, Mark, and Lars Isaksen, 2000, Ku-Band Scatterometer Data Assimilation, paper submitted to the Quarterly J. Royal meteorol. Soc.

Le Meur, Didier, Lars Isaksen, and Ad Stoffelen, "Impact of ERS-1/ERS-2 scatterometer tandem on the ECMWF 3D-var assimilation system", Proc. Of the third ERS symposium – space at the service of our environment, Florence, 17-21 March 1997, ESA special report, ESTEC, Noordwijk, the Netherlands, 1997.

Le Meur, Didier, Lars Isaksen, Ad Stoffelen, 1998, "Wind speed calibration of ERS scatterometer data for assimilation purposes at ECMWF", proc. CEOS Wind and Wave validation Workshop, held at ESTEC, Noordwijk, the Netherlands from 3-5 June 1997.

Lorenc, A. C., 1988, Optimal nonlinear analysis, Quart. J. Royal Meteor. Soc. **114**, pp. 205-240.

Mastenbroek, C., 1996, Wind-Wave Interaction, thesis at the Delft University of Technology, Delft, the Netherlands, 12 Dcember 1996.

Portabella, Marcos, and Ad Stoffelen, EUMETSAT QuikSCAT Fellowship Progress Report, KNMI, de Bilt, the Netherlands, 2000.

Portabella, Marcos, and Ad Stoffelen, 2000, On Quality Control and Rain Detection of SeaWinds, J. Atmosph. Oceanic Technol., accepted.

Rohn, M., G. Kelly, and R. Saunders, 1999, Experiments with Atmospheric Motion Vectors at ECMWF, in Proc. of Fourth International Winds Workshop held 19-23 October 1998, EUMETSAT P24, ISSN 1023-0416, pp. 139-146.

SSMIS, 2000, http://xenon.aerojet.com/Weapon_Systems/Earth_Sensing/SSMIS/

Stoffelen, Ad, 1999, A Simple Method for Calibration of a Scatterometer over the Ocean, J. Atm. and Ocean Techn. 16(2), 275-282; Appendix A of Stoffelen (1998a).

Stoffelen, Ad, 1998a, Scatterometry, PhD thesis, ISBN 90-393-1708-9, http://pablo.ubu.ruu.nl/~proefsch/01840669/inhoud.htm.

Stoffelen, Ad, 1998b, Error modeling and calibration; towards the true surface wind speed, J.Geoph. Res. 103 (C4), 7755-7766; Chapter IV of Stoffelen (1998a).

Stoffelen, Ad, 1997, Calibration and validation in the backscatter domain, proc. CEOS Wind and Wave validation Workshop, held at ESTEC, Noordwijk, the Netherlands from 3-5 June 1997.

Stoffelen, A. C. M. and D. L. T. Anderson, 1997a, Scatterometer Data Interpretation: Measurement Space and Inversion, J. Atmosph. and Ocean Techn. 14 (6), 1298-1313; Chapter II of Stoffelen (1998a).

Stoffelen, A. C. M. and D. L. T. Anderson, 1997c, Ambiguity removal and assimilation of scatterometer data, Q. J. Roy. Meteorol. Soc., 123, 491-518; Chapter V of Stoffelen (1998a).

Stoffelen, A. C. M. and D. L. T. Anderson, 1993, Wind retrieval and ERS-1 radar backscatter measurements, Adv. Space Res. 13 (5), pp. (5)53-(5)60.

Stoffelen, Ad and Paul van Beukering, 1997, The impact of improved scatterometer winds on HIRLAM analyses and forecasts, BCRS study contract 1.1OP-04, report published by BCRS,

Delft, The Netherlands, and HIRLAM technical report #31, published by IMET, Dublin, Ireland.

Stoffelen, Ad, Aart Voorrips, and John de Vries, Towards the Real-Time Use of QuikScat Winds, draft BCRS project report, available from author.

Tahara Y., 2000, The preliminary Impact Study of Using QuikScat/SeaWinds Ocean Surface Winds on the JMA Global Model, Proc. Fifth International Winds Workshop held 28 Feb. -3 March 2000 in Lorne Australia, to be published by EUMETSAT.

Vries, de, John, and Ad Stoffelen, 2000, 2D variational ambiguity removal, Project report for the BCRS, KNMI, de Bilt, the Netherlands.

Wentz, F. J., S. Peteherych and L. A. Thomas, A model function for ocean radar cross sections at 14.6 GHz, J. Geophys. Res., 89, pp. 3689-3704, 1984.

WindSat, 2000, http://www.pxi.com/windsat/summary.html

WMO, 2000, minutes of meeting on 1999 French Christmas storms.

11 ACRONYMS

2D-VAR	2-dimensional AR
3D-Var	3-dimensional variational meteorological analysis
4D-Var	Variational meteorological analysis in space and time
ADEOS-I	Advanced Earth Observation System (1996-7)
ADEOS-II	Advanced Earth Observation System (2002)
AMSR	Advanced Microwave Instrument on ADEOS-II
AR	Ambiguity Removal
ASCAT	Advanced scatterometer on METOP
BCRS	Beleidscommissie Remote Sensing (Dutch)
BUFR	Binary Universal Format Representation
ECMWF	European Centre for Medium-range Weather Forecasts
ERS	European Remote Sensing Satellite
ESA	European Space Agency
EUMETSAT	European Organisation for the Exploitation of Meteorological Satellites
GMF	Geophysical Model Function
GMT	Greenwich time
HH	Horizontal polarisation emitted-Horizontal received
HIRLAM	HIgh-Resolution Limited-Area Model
JPL	Jet Propulsion Laboratory
KNMI	Royal Netherlands Meteorological Institute
METOP	Meteorological Operational satellite (2003)
MLE	Maximum Likelihood Estimator
NASA	National Aeronautics and Space Administration (USA)
NCEP	National Centre for Atmospheric Prediction (USA)
NOAA	National Oceanographic and Atmospheric Administration (USA)
NRMS	Normalised RMS
NRSP	National Remote-Sensing Programme (Dutch)
NSCAT	NASA Scatterometer
NWP	Numerical Weather Prediction
OI	Optimal (statistical) Interpolation

PreScat	Processor of ERS scatterometer data at KNMI
QC	Quality Control
QuikScat	NASA scatterometer mission with SeaWinds
RMS	Root-Mean-Squared
SAF	EUMETSAT Satellite Application Facility
SAG	Science Advisory Group
SD	Standard Deviation
SDE	Standard Deviation of Error
SeaWinds	NASA rotating pencil-beam scatterometer
SNR	Signal-to-Noise Ratio
SSMI	Special Sensor Microwave Imager
SSMIS	SSMI and Sounder
SWVC	Super WVC
VV	Vertical polarisation emitted-Vertical received
WMO	World Meteorological Organisation
WVC	Wind Vector Cell

12 ACKNOWLEDGEMENTS

ESA, NASA and NOAA are acknowledged for providing data and help using it, and the SeaWinds and ASCAT project and science teams for their inspiring meetings. The collaboration with ECMWF, and more in particular Mark Leidner, on visit from AER, Lars Isaksen and Didier Le Meur has proven very fruitful over the years. The KNMI scatterometer science team (http://www.knmi.nl/scatterometer) as referred to several times in this paper is indispensible for cherishing and extending the expertise in the use of scatterometer data.